

# RSC Sustainability



**Accepted Manuscript** 

This article can be cited before page numbers have been issued, to do this please use: E. F. CLARK, T. CHHABRA, Q. ZHOU, N. Lorenz, J. WOODS, P. Van Puyvelde, B. Kumru and B. Sels, *RSC Sustainability*, 2025, DOI: 10.1039/D5SU00828J.



This is an Accepted Manuscript, which has been through the Royal Society of Chemistry peer review process and has been accepted for publication.

Accepted Manuscripts are published online shortly after acceptance, before technical editing, formatting and proof reading. Using this free service, authors can make their results available to the community, in citable form, before we publish the edited article. We will replace this Accepted Manuscript with the edited and formatted Advance Article as soon as it is available.

You can find more information about Accepted Manuscripts in the <u>Information for Authors</u>.

Please note that technical editing may introduce minor changes to the text and/or graphics, which may alter content. The journal's standard Terms & Conditions and the Ethical guidelines still apply. In no event shall the Royal Society of Chemistry be held responsible for any errors or omissions in this Accepted Manuscript or any consequences arising from the use of any information it contains.



View Article Online

DOI: 10.1039/D5SU00828J

## **Sustainability Spotlight Statement**

This work present a simple and detailed study on epoxy resins prepared entirely from bio-based lignin oil and epoxidized soybean oil. These materials replace the toxic, non-recyclable bisphenol A and epichlorohydrin traditionally derived from petrochemical sources. Our vitrimers system utilizes lignin oil with inherently sufficient phenolic and aliphatic hydroxyl groups, eliminating additional functionalization steps. This simplifies the overall process, reducing both cost and time requirements. Our future research will focus on exploring variations in lignin oil composition and their reactivity toward epoxy resins, with particular emphasis on enhancing sustainability and minimizing waste generation during epoxy resin preparation.

# **Vitrimers from Non-Functionalized Lignin Oil**

View Article Online DOI: 10.1039/D5SU00828J

# and Epoxidized Soybean Oil

Ella F. Clark, <sup>†a</sup> Tripti Chhabra, <sup>†a</sup> Qianxiang Zhou, <sup>a</sup> Niklas Lorenz, <sup>b</sup> Jonathan Woods, <sup>a</sup> Peter Van Puyvelde, <sup>c</sup> Baris Kumru <sup>b</sup> and Bert F. Sels <sup>a</sup>

<sup>a</sup>Center For Sustainable Catalysis and Engineering, Department of Microbial and Molecular Systems, KU Leuven, Leuven, Belgium

<sup>b</sup>Faculty of Aerospace Engineering, Aerospace Structures & Materials Department, Delft University of Technology, 2629 HS Delft, Netherlands

<sup>c</sup>Department of Chemical Engineering, Soft Matter, Rheology and Technology (SMaRT), KU Leuven, Celestijnenlaan 200F, 3001 Leuven, Belgium

[†] These authors contributed equally to this work.

\*Corresponding authors

#### **Abstract**

This study reports the development of fully bio-based epoxy resins containing dynamic ester bonds capable of transesterification at 100 °C. The inherent functionality of the lignin oil derived from reductive catalytic fractionation (RCF) biorefinery process, enables effective curing with epoxidized soybean oil, eliminating the need for additional treatments. The resulting epoxy resins shows similar thermochemical behavior for both pristine and reprocessed epoxy resins. This work highlights a sustainable and efficient route for producing reprocessable vitrimers using non-functionalized lignin oil.

## Introduction

Epoxy resins are a class of thermoset materials with a wide application scope, such as in household items, aerospace, transportation, infrastructure and electrical equipment.<sup>1,2</sup> This is due to their excellent properties, namely high chemical resistance,

thermal stability and mechanical strength and suitability for electrical insulation. Of the 10008283 derived from petroleum sources, their inert cross-linked structure does not allow for reprocessing, recycling or degradation. To move towards a more sustainable material whilst maintaining the desirable properties, bioderived monomers with low toxicity must be used to create a material capable of being reprocessed. Covalent adaptable networks (CAN) possess dynamic covalent bonds, which can be broken and reformed, resulting in a material with macroscopic flow capable of being reprocessed. Dynamic bonding, such as transesterification, can be introduced into epoxy resins through the choice of hardener to form a vitrimer. The example, Ju and co-workers reacted tannic acid with epoxidized vegetable oils to produce epoxy resins with good reprocessibility and robust mechanical properties. 14

Biomass is currently the most abundant renewable and biodegradable resource on our planet and a good alternative to petroleum based products. 15 Lignin is the second most abundant polymer present in biomass. It is naturally rich in aromatic units, which are present in plant structures. 16-18 Numerous chemical process have been extensively studied for the isolation of lignin from the lignocellulose biomass. Kraft, sulfite, alkaline and klason lignin are typically obtained from the pulping methods. While these processes yield high quality cellulose, the lignin produced is highly modified from its native structure due to harsh chemicals treatment. Milled wood lignin, obtained by intensive grinding followed by solvent treatment, also results in structurally altered lignin. The organosoly process and ionic liquid method are also used to obtained lignin. In organosolv process, structurally modified lignin is observed if treated with high temperature and ionic liquid method is not cost effective. 19 Therefore, the valorization of lignocellulose biomass to obtain structurally unmodified lignin in an economically viable manner remains a significant challenge.<sup>20</sup> Reductive catalytic fractionation (RCF) is a promising one pot technique and is often referred to as a "lignin first-biorefinery" approach. The RCF process enables the efficient separation of carbohydrate pulp and lignin oil through a straightforward chemical process. Lignin oil obtained via RCF comprises a mixture of phenolic monomers, dimers and oligomers, preserving lignin in its native and unaltered form. 19,21

The dynamic structure of lignin consist of different active functional groups such as hydroxyl, methoxy, aldehyde and carboxylic. This allows lignin to undergo a range of

chemical modifications such as alcoholysis, oxidation, reduction, epoxidation, via position oxidation, reduction, epoxidation of light demethoxylation. This modified structure of light can be used to develop new materials with improved reprocessability, improved mechanical properties, and environmental sustainability. The control oxidation oxidation, reduction, epoxidation, via position oxidation, reduction, epoxidation oxidation, reduction, epoxidation, via position oxidation, reduction, epoxidation, via position oxidation, reduction, epoxidation, via position oxidation oxidation

Zhang and coworkers used the commercially available kraft lignin which was further subjected to ozone oxidation for cleavage of lignin structure and also to increase the carboxylic groups in the lignin. The modified lignin was used to prepare the vitrimers with sebacic acid for reprocessable adhesives.<sup>24</sup> Recently, Duval *et al.* used the commercial kraft lignin and treated it with ethylene carbonate to increase the aliphatic hydroxyl groups present in the lignin. The modified kraft lignin was further crosslinked with poly(ethylene glycol) bis(carboxymethyl) ether to form lignin based polyester networks.<sup>25</sup> Wang *et al.*<sup>26</sup> reported the development of epoxy resins from kraft lignin and epoxidized soybean oil (ESO). However, the inherent polarity and hydrophilicity of lignin, opposes the hydrophobic nature of ESO which leads to a compatibility issue. To enhance the compatibility between lignin and ESO, lignin underwent esterification with tung oil anhydride to enhance its compatibility with ESO prior to epoxy resin synthesis. There is a need to prepare the structurally unmodified lignin with high phenolic and aliphatic hydroxyl content for the synthesis of vitrimers materials.

This work explores the potential of unmodified lignin oil obtained from RCF<sup>21,27</sup>— an emerging lignocellulose biorefinery that focusses on extraction of high quality lignin oil, to develop sustainable and bio based epoxy vitrimers (Scheme 1). The aliphatic and phenolic OH present in the lignin oil is reacted with ESO to form an epoxy resins. Once cured, these resins resulted in bio-based thermosets which are studied for their dynamic bonding and reprocessibility.

View Article Online

DOI: 10.1039/D5SU00828J

#### Results and discussion

**Scheme 1**: Illustration of the reaction between LO and ESO with Al(OTf)<sub>3</sub> at 90 °C, resulting in an epoxy resin. Dynamic bonding occurs between ester and alcohol groups (transesterification), catalyzed by Al(OTf)<sub>3</sub> at 100 °C.

Lignin oil, rich in both aliphatic and phenolic hydroxyl groups, was obtained *via* the RCF process and used directly without further chemical modification (See Supporting Information for details). The weight-average molar mass ( $M_w$ ) of LO was found to be 2159 g mol<sup>-1</sup> determined from GPC as shown in Figure S1. The quantitative analysis of aliphatic and phenolic hydroxyl groups present in LO was determined by <sup>31</sup>P{<sup>1</sup>H} NMR analysis. The G unit (Guaiacyl), S unit (Syringyl) along with condensed structures and H unit (hydroxyphenyl) were calculated to be 0.82 mmol g<sup>-1</sup>, 1.94 mmol g<sup>-1</sup> and 0.13 mmol g<sup>-1</sup> respectively. The total amount of aliphatic and phenolic hydroxylic groups was found to be 1.94 mmol g<sup>-1</sup> and 2.89 mmol g<sup>-1</sup>, respectively. The 2D  $^{1}$ H –  $^{13}$ C HSQC NMR spectra was further used to elucidate the fragments and its relative percentage present in the LO as presented in Figure 1 (a, b, e) measured in DMSO-d<sub>6</sub>. The main structural units found in LO are Me, E, P with the relative amount of 0.6%, 13.4%, 12.7% respectively. The P  $\gamma$ -OH structural unit was found to be 29.8% which confirms a high aliphatic hydroxyl group content in the LO. The other structures present in LO was P  $\gamma$ -OMe (8.8%),  $\alpha$ ,  $\beta$   $\beta$ -1E (3.6%) along with -OCH<sub>3</sub> and ROOCH<sub>3</sub> functional groups.<sup>28</sup>

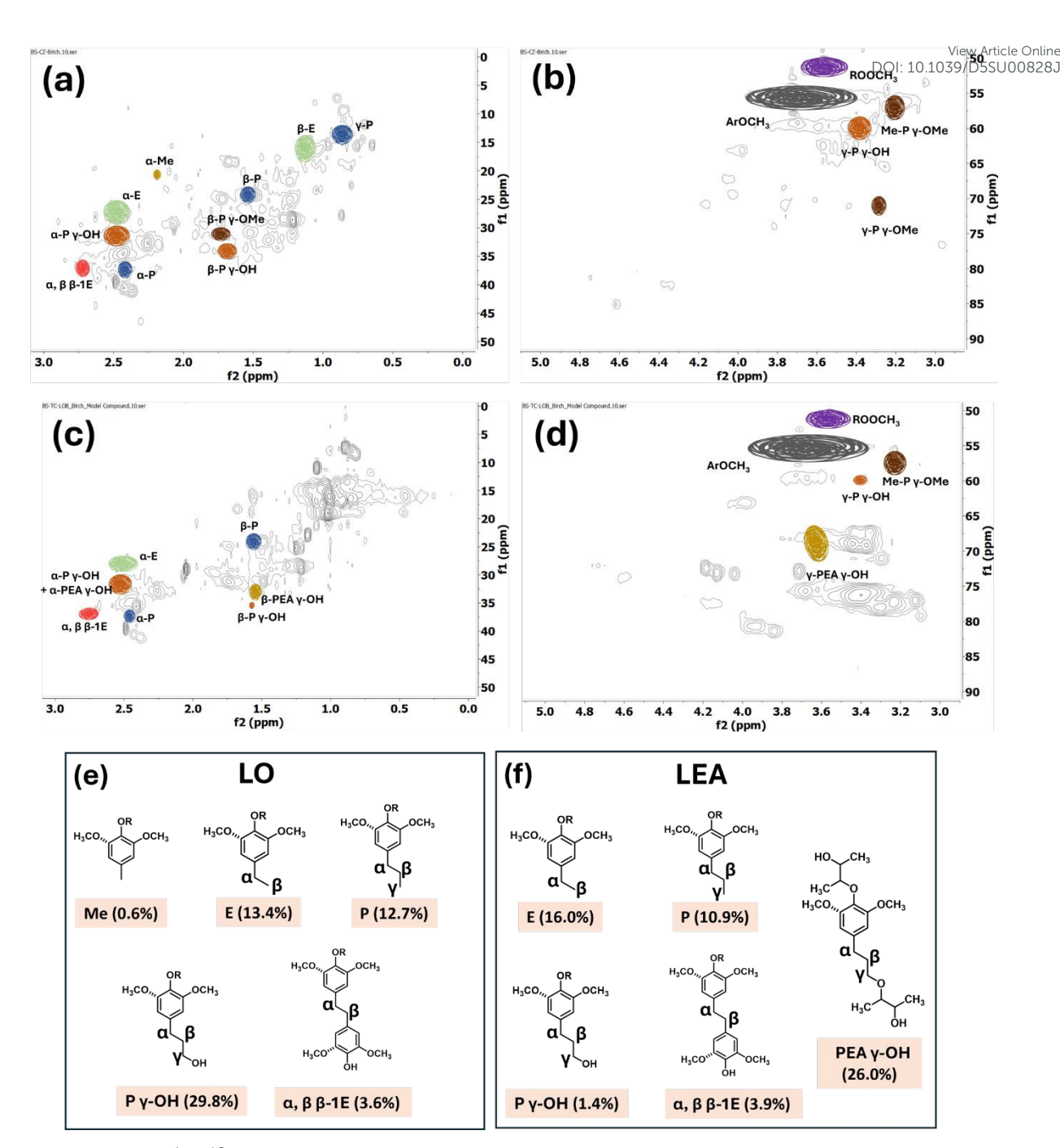


**Figure 1**. 2D (<sup>1</sup>H-<sup>13</sup>C) HSQC NMR spectra of (a, b) LO, (c, d) LEA. Relative quantification of structures in (e) LO and (f) LEA.

The optimization of curing ESO with LO was next carried out. Catalyst screening was performed *via* DSC analysis, identifying curing by measuring exothermic events caused by the ring-opening of the epoxide. Analysis was done at a weight/weight% ratio (w/w%) of LO/ESO of 24% and catalyst/ESO w/w% of 1% to ensure the epoxide was in excess. Three catalysts, zinc acetate (ZnAc<sub>2</sub>), aluminium trifluoromethanesulfonate Al(OTf)<sub>3</sub> and histidine, were all chosen, having all been reported to catalyse epoxy curing and dynamic ester exchange.<sup>8,29–31</sup>

Although ZnAc<sub>2</sub> produced a minor exothermic event, the largest exotherm was produced a minor exothermic event, the largest exotherm was produced a minor exothermic event, the largest exotherm was produced a minor exothermic event, the largest exotherm was produced a minor exothermic event, the largest exotherm was produced a minor exothermic event, the largest exotherm was produced a minor exothermic event. Al(OTf)<sub>3</sub> with a peak exothermic temperature at 109 °C (Figure S4). Film formulation was next optimized in a PTFE mold. Initial upscaling was done with 2.00 g of ESO with w/w% of LO/ESO of 24% and Al(OTf)<sub>3</sub>/ESO w/w % of 1% at 90 °C in an oven. The temperature was varied across the exothermic range from 120 - 90 °C (Table 1, Entries 1-3). Curing at 90 °C produced a homogeneous film unlike higher temperatures in which bubbling occurred, likely due to rapid curing. After 22 h, the film had solidified and was removed from the mold. The disappearance of the epoxy  $v_{\text{C-O}}$  vibration between 800 – 850 cm<sup>-1</sup> in the FT-IR spectrum suggested high consumption of epoxy groups (Figure S7). No residual curing exotherm was observed for any of the films after curing, confirming all films were fully cured. Solidification occurred after only 1 hour and FT-IR analysis confirmed the film was fully cured. The catalyst loading was further decreased to 0.5 and 0.25 Al(OTf)<sub>3</sub>/ESO w/w% (Table 1, Entries 7-9). Curing occurred at all loadings evidenced by solidification and the disappearance of the  $v_{C-O}$  vibration in the FT-IR spectrum. A significant increase in  $T_{d,5\%}$  with decreased catalyst loading was observed suggesting Al(OTf)<sub>3</sub> catalyzes the degradation of the epoxy resin. Finally, the w/w% of LO/ESO was varied (Table 1, Entries 9 and 10). The  $T_{\rm d,5\%}$  decreased with increasing lignin content (Figure S5) with the  $T_{\rm g}$  remaining between -36 and -32 °C. The DSC trace of all films also exhibited an endotherm between -20 and 0 °C which was attributed to the melting of ESO (Figure S6).

Table 1. Film Optimization.

Entry <sup>a</sup>	LO/ESO w/w %	Cure time (h)	Cure Temp (°C)	cat/ESO w/w %	$T_{g}^{b}$	T <sub>d,5%</sub> <sup>c</sup>
_	•	22	100	4.00	20	222
1	24	22	120	1.00	<b>-</b> 39	239
2	24	22	105	1.00	-38	241
3	24	22	90	1.00	-35	228
4	24	5	90	1.00	-36	219
5	24	3	90	1.00	-40	195
6	24	1	90	1.00	-43	206
7	24	22	90	0.50	-36	243
8	24	22	90	0.25	-34	266
9	18	4	90	0.50	-37	222
10	28	4	90	0.50	-35	224
11	24	22	90	0	-	-
12	24	28	180	0	-	-

<sup>&</sup>lt;sup>a</sup> Reactions carried out with Al(OTf)<sub>3</sub>. <sup>b</sup> Values taken from second heating cycle. <sup>c</sup> Value taken at 5 % mass loss.

To gain further insights into the resin formulation, trans-2,3-epoxybutane was chose of a contraction of LO and epoxide. Studying the reaction of LO with trans-2,3-epoxybutane helps in identifying which functional groups present in LO participate in the curing reaction. The chemical reaction between LO and trans-2,3-epoxybutane resulted in the lignin-epoxy adduct (LEA). The formation of LEA resulted in an increase in  $M_{\rm w}$  from 2159 g mol<sup>-1</sup> to 3385 g mol<sup>-1</sup>, as shown in Figure S1, indicating that the epoxide has successfully reacted with the lignin oil. The <sup>31</sup>P{<sup>1</sup>H} NMR analysis confirms an increase in aliphatic hydroxyl content from 1.94 mmol g<sup>-1</sup> in LO to 2.61 mmol g<sup>-1</sup> in LEA, as shown in Figure S2 and Table S1. A corresponding decrease from 2.89 mmol g<sup>-1</sup> to 1.02 mmol g<sup>-1</sup> in phenolic hydroxyl groups was also observed, signifying addition of trans-2,3-epoxybutane at phenolic position results in the formation of aliphatic hydroxyl group. These observations suggest that the epoxide reacts with both aliphatic and phenolic hydroxyl functional groups, which are present among the various structural motifs present in lignin oil.

Furthermore, propanol guaiacol (PG) was chosen as model compound for lignin to understand the reactivity of epoxide with aliphatic hydroxyl and phenolic groups present in LO. PG was next reacted with trans-2,3-epoxybutane to form PG-epoxy adduct (PGEA) as a model product.  $^1\text{H}-^{13}\text{C}$  HSQC and relative quantification for the of PGEA are provided in Figure S2 and Table S2.  $^1\text{H}-^{13}\text{C}$  HSQC of PGEA shows that signal for the  $\alpha$ -position of both PG and PGEA remained at 2.5 ppm, whereas a shift in the signals corresponding to the  $\beta$  and  $\gamma$ -position was observed for PG and PGEA which confirms the addition of trans-2,3-epoxybutane and also provide the relative quantification of epoxidation. PGEA<sub>1</sub>, PGEA<sub>2</sub> were attributed to the addition of trans-2,3-epoxybutane at the phenolic hydroxyl position and PGEA<sub>3</sub>, PGEA<sub>4</sub> were attributed to the addition of trans-2,3-epoxybutane at the aliphatic hydroxyl position. The higher relative percentages of PGEA<sub>3</sub> and PGEA<sub>4</sub> compared to PGEA<sub>1</sub> and PGEA<sub>2</sub> (Table S2) suggest that addition of trans-2,3-epoxybutane is more favorable at aliphatic hydroxyl sites than at phenolic positions.

The  $^1\text{H}-^{13}\text{C}$  HSQC spectra and relative quantification of LEA are shown in Figure 1 (c, d, f). Signals for the  $\alpha$ -position in both P  $\gamma$ -OH and PEA  $\gamma$ -OH appear at the same location, while the  $\beta$  and  $\gamma$ -positions for P  $\gamma$ -OH and PEA  $\gamma$ -OH differ, enabling the calculation of the extent of trans-2,3-epoxybutane addition. The relative amount of P  $\gamma$ -OH decreases from 29.8% to 1.4%, while PEA  $\gamma$ -OH accounts for 26.0%, which confirms the successful addition on the lignin

oil. However, due to signal clustering in the PEA y-OH region, specific assignments uncertain. Unlike the clear preference for addition of trans-2,3-epoxybutane at aliphatic hydroxyl groups observed in PG-epoxy adduct, the data for lignin-epoxy adduct do not allow for a definitive conclusion regarding the reactivity of aliphatic versus phenolic hydroxyl groups. The chemical reactivity of trans-2,3-epoxybutane with PG and LO indicates that addition of epoxy functional groups takes place at both aliphatic and phenolic positions in various structures present in lignin oil, with higher reactivity observed at the aliphatic position compared to the phenolic position.

## **Dynamic Bond Exchange**

Vitrimers show that the stress caused by deformation can be released at high temperatures through dynamic cross-linking exchange. To establish whether the network behaves as a vitrimer, shear stress-relaxation experiments were performed between 110 and 140 °C on an epoxy resin (w/w% of LO/ESO of 24% and Al(OTf)<sub>3</sub>/ESO w/w % of 1%, cured at 90 °C). The shear relaxation modulus G(t) was measured as a function of time at each temperature. A decrease in relaxation time was observed as the temperature was increased from 110 to 140 °C (Figure 2a). Normalized shear modulus data were approximated by Kohlrausch-Williams-Watts stretched exponential decay to obtain average relaxation times  $\langle \tau \rangle$  (refer to SI).<sup>32,33</sup> Low values of  $\langle \tau \rangle$  (Figure S12) indicate a rapid stress relaxation behaviour and excellent dynamic properties while stretching coefficient  $\beta$  values ranging from 0.35 to 0.38 propose an inhomogeneous relaxation process which may be attributed to the inhomogeneous structure of LO. For the LO derived epoxy resins,  $\langle \tau \rangle$  was shown to be less than 600 seconds at 140 °C, with activation energies of 112 KJ mol<sup>-1</sup>, which falls within the range of transesterification vitrimers<sup>34,35</sup> between 85–129 kJ mol<sup>-1</sup>.

View Article Online DOI: 10.1039/D5SU00828J

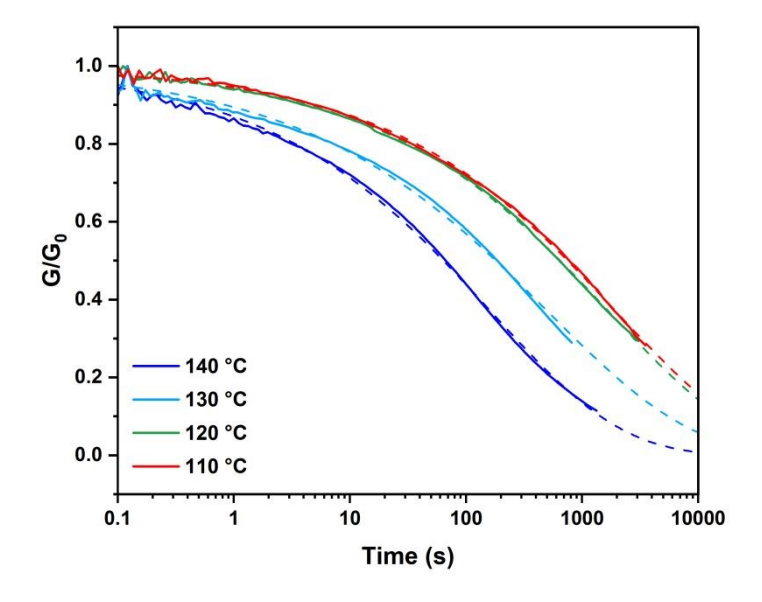


**Figure 2**. Normalized relaxation modulus (solid line) and approximation by Kohlrausch–Williams–Watts function (dotted line) at different temperatures.

The reprocessing capability was next explored. An epoxy resin was formulated at a w/w% of LO/ESO of 24% and Al(OTf)<sub>3</sub>/ESO w/w % of 1% at 90 °C. A fracture was introduced into the epoxy resin using a knife, and subsequently characterized using Scanning Electron Microscopy (SEM) Figure 3(a, b). Following compression molding at 100 °C for 3 h at 50 bar of pressure, no fracture was observed *via* SEM demonstrating the film's ability to be reprocessed Figure 3(c, d).

The reprocessability of one of the epoxy resins was next assessed by breaking the sample into pieces, followed by compression molding the pieces, at 100 °C for 3 h after which the film was reformed (Figure S13). Samples for Dynamic Mechanical Analysis (DMA) were prepared by cleaving a 62.5 x 12.5 mm bar in two followed by compression molding at 100 °C for 3 h. These were compared to pristine samples (uncut, cured epoxy resins) of the same dimension. Figure 3e shows the temperature-dependent modulus of the pristine and reprocessed samples, confirming similar thermomechanical behavior of both samples. A broad glass transition temperature,  $T_g$ , of -7.5 °C ( $\tan(\delta)$  peak value) remains constant before and after the thermal-induced healing process, excluding any undesired degradation by bond breakage during reprocessing, which would manifest in decreasing  $T_g$  values. <sup>36,37</sup> The master curves of the pristine and reprocessed material at a reference temperature of 20 °C (Figure S14) shows similar behavior of both over a wide temperature and frequency range, indicating

preservation of thermomechanical properties during the healing cycle. Furthermore, the structure of pristine factors  $a_T$  derived from the loss factor tan  $\delta$  (Figure S15) confirm similar behavior of pristine and reprocessed samples. This shows the overall viscoelastic response of the reprocessed specimen does not significantly differ between the pristine and reprocessed sample. Moreover, the glassy regime falls within the range of similar epoxy vitrimers derived from functionalized lignin<sup>25,38–40</sup> as well as existing commercial epoxy resins.

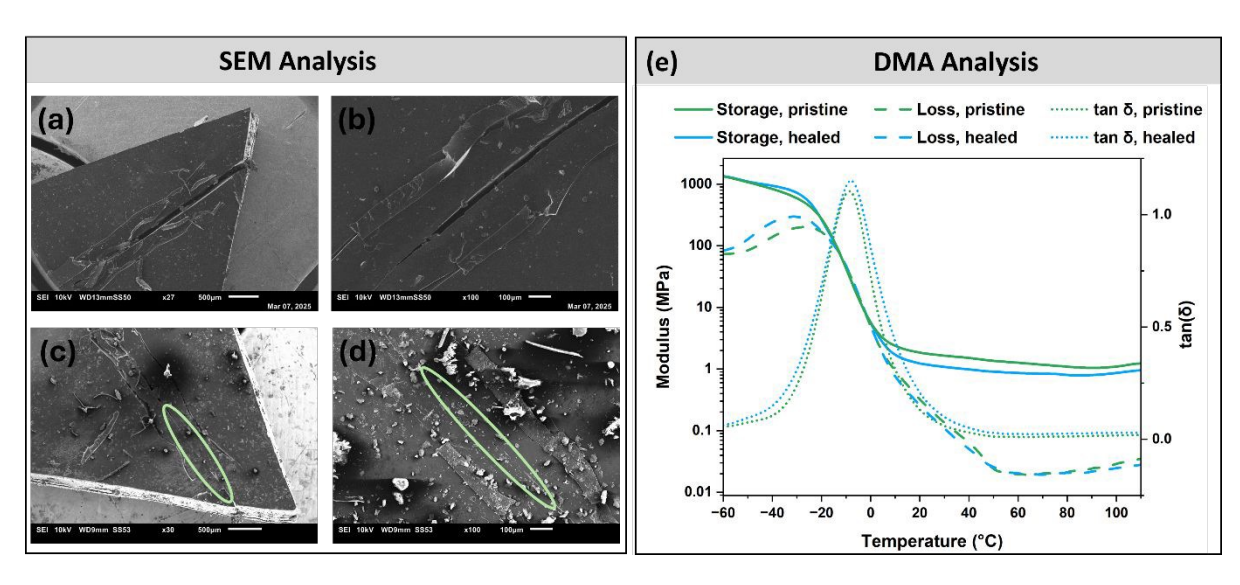


**Figure 3.** SEM images of (a, b) freshly cut polymeric film and (c, d) compression molded polymeric film. The scale bars for the SEM images are 500  $\mu$ m for (a, c) and 100  $\mu$ m for (b, d). (e) Time-dependent modulus development of pristine and reprocessed sample.

# Conclusions

The formulation of fully biobased epoxy resins from unfunctionalized LO and ESO has been reported. DSC curing analysis found  $AI(OTf)_3$  to be an effective catalyst which was further corroborated by  $^{31}P\{^1H\}$  and  $^1H-^{13}C$  HSQC NMR analysis which showed  $AI(OTf)_3$  catalyzed the ring-opening attack of epoxides by LO, with preference to aliphatic alcohol groups. Having optimized film formulation, rheology, SEM and DMA experiments were then performed to show these epoxy resins undergo dynamic bond exchange and are capable of being reprocessed with pristine and reprocessed films exhibiting the same viscoelastic properties.

View Article Online

DOI: 10.1039/D5SU00828J

## **Data availability**

All data supporting the findings of this study are available. All the findings are included in the article and its supporting information. Full experimental procedures are provided in the supporting information.

#### **Conflicts of interest**

There are no conflicts to declare.

## Acknowledgements

This project has received financial support from Internal KU Leuven research fund for the GORILLA project (C2M/23/025), FWO Strategic research project LigDYN (S000724N) and Next-BIOREF (IBOF/21/105).

#### References

- 1 Y. Jiang, J. Li, D. Li, Y. Ma, S. Zhou, Y. Wang and D. Zhang, *Chem. Soc. Rev.*, 2024, **53**, 624–655.
- 2 A. Shundo, S. Yamamoto and K. Tanaka, *JACS Au*, 2022, **2**, 1522–1542.
- 3 M. Peerzada, S. Abbasi, K. T. Lau and N. Hameed, *Ind. Eng. Chem. Res.*, 2020, **59**, 6375–6390.
- 4 C. J. Kloxin and C. N. Bowman, *Chem. Soc. Rev.*, 2013, **42**, 7161–7173.
- Biobased covalent adaptable networks: towards better sustainability of thermosets., https://pubs.rsc.org/en/content/articlehtml/2022/gc/d2gc01325h, (accessed May 26, 2025).
- 6 F. Zhang, L. Zhang, M. Yaseen and K. Huang, J. Appl. Polym. Sci., 2021, **138**, 50260.
- P. Verdugo, D. Santiago, S. De la Flor and À. Serra, *ACS Sustain. Chem. Eng.*, 2024, **12**, 5965–5978.

2025. Downloaded on 08/11/25 17:59:39.

Open Access Article. Published on 31

- Y. Tao, L. Fang, M. Dai, C. Wang, J. Sun and Q. Fang, *Polym. Chem.*, 2020, 11, 45000 SSU008283
- 9 E. Albertini, S. Dalle Vacche, R. Bongiovanni, I. Bianco, G. A. Blengini and A. Vitale, *ACS Sustain. Chem. Eng.*, 2025, **13**, 2120–2131.
- 10 M. Comí, B. Van Ballaer, J. Gracia-Vitoria, D. Parida, A. Aerts, K. Vanbroekhoven and R. Vendamme, *ACS Sustain. Chem. Eng.*, 2024, **12**, 9279–9289.
- 11 H. Yao, H. Yang, L. Jiang, W. Huang, Q. Jiang, B. Jiang and G. Zhang, *RSC Appl. Polym.*, 2025, **3**, 163–172.
- 12 J. Zhang, Z. Gong, C. Wu, T. Li, Y. Tang, J. Wu, C. Jiang, M. Miao and D. Zhang, *Green Chem.*, 2022, **24**, 6900–6911.
- D. Montarnal, M. Capelot, F. Tournilhac and L. Leibler, Science, 2011, 334, 965–968.
- 14 J. Li, B. Ju and S. Zhang, *Green Chem.*, 2024, **26**, 7113–7122.
- 15 B. H. H. Goh, H. C. Ong, M. Y. Cheah, W.-H. Chen, K. L. Yu and T. M. I. Mahlia, *Renew. Sustain. Energy Rev.*, 2019, **107**, 59–74.
- Lignin Valorization: Improving Lignin Processing in the Biorefinery | Science, https://www.science.org/doi/full/10.1126/science.1246843, (accessed May 26, 2025).
- 17 E. Sheridan, S. Filonenko, A. Volikov, J. Antti Sirviö and M. Antonietti, *Green Chem.*, 2024, **26**, 2967–2984.
- 18 Y. Liao and B. F. Sels, *Lignin chemistry: characterization, isolation, and valorization,* John Wiley & Sons, 2024.
- 19 Z. Sun, B. Fridrich, A. de Santi, S. Elangovan and K. Barta, *Chem. Rev.*, 2018, **118**, 614–678.
- 20 Y. Huang, Y. Duan, S. Qiu, M. Wang, C. Ju, H. Cao, Y. Fang and T. Tan, *Sustain. Energy Fuels*, 2018, **2**, 637–647.
- S. Van Den Bosch, W. Schutyser, R. Vanholme, T. Driessen, S.-F. Koelewijn, T. Renders, B. De Meester, W. J. J. Huijgen, W. Dehaen, C. M. Courtin, B. Lagrain, W. Boerjan and B. F. Sels, *Energy Environ. Sci.*, 2015, **8**, 1748–1763.

- 22 N. Sun, Z. Wang, X. Ma, K. Zhang, Z. Wang, Z. Guo, Y. Chen, L. Sun, W. Luand Yang Grand Crops Prod., 2021, **174**, 114178.
- 23 R. Tang, B. Xue, J. Tan, Y. Guan, J. Wen, X. Li and W. Zhao, *ACS Appl. Polym. Mater.*, 2022, **4**, 1117–1125.
- 24 S. Zhang, T. Liu, C. Hao, L. Wang, J. Han, H. Liu and J. Zhang, *Green Chem.*, 2018, **20**, 2995–3000.
- 25 A. Duval, W. Benali and L. Avérous, *Green Chem.*, 2024, **26**, 8414–8427.
- 26 X. Zhen, X. Cui, A. A. N. M. Al-Haimi, X. Wang, H. Liang, Z. Xu and Z. Wang, *Int. J. Biol. Macromol.*, 2024, **254**, 127760.
- 27 M. Chen, Y. Li, F. Lu, J. S. Luterbacher and J. Ralph, *ACS Sustain. Chem. Eng.*, 2023, **11**, 10001–10017.
- 28 K. V. Aelst, E. V. Sinay, T. Vangeel, E. Cooreman, G. V. den Bossche, T. Renders, J. V. Aelst, S. V. den Bosch and B. F. Sels, *Chem. Sci.*, 2020, **11**, 11498–11508.
- 29 D. B. G. Williams and M. Lawton, *Org. Biomol. Chem.*, 2005, **3**, 3269–3272.
- 30 I. D. S. Silva, P. Moerbitz, I. Bretz, J. V. Barreto, A. Ries, C. B. B. Luna, E. M. Araújo and R. M. R. Wellen, *J. Appl. Polym. Sci.*, 2025, **142**, e56908.
- 31 M. Shibata, J. Fujigasaki, M. Enjoji, A. Shibita, N. Teramoto and S. Ifuku, *Eur. Polym. J.*, 2018, **98**, 216–225.
- 32 G. Williams and D. C. Watts, *Trans. Faraday Soc.*, 1970, **66**, 80–85.
- Exploring the Cure State Dependence of Relaxation and the Vitrimer Transition Phenomena of a Disulfide-Based Epoxy Vitrimer, https://onlinelibrary.wiley.com/doi/epdf/10.1002/pol.20250463, (accessed September 30, 2025).
- 34 M. Chen, H. Si, H. Zhang, L. Zhou, Y. Wu, L. Song, M. Kang and X.-L. Zhao, *Macromolecules*, 2021, **54**, 10110–10117.
- 35 M. Capelot, M. M. Unterlass, F. Tournilhac and L. Leibler, *ACS Macro Lett.*, 2012, **1**, 789–792.

- N. Lorenz, W. E. Dyer and B. Kumru, ACS Appl. Polym. Mater., 2025, 7, 1934; 1946; Article Online Online Online
- A. Ruiz de Luzuriaga, N. Markaide, A. M. Salaberria, I. Azcune, A. Rekondo and H. J. Grande, *Polymers*, 2022, **14**, 3180.
- 38 F. Meng, M. O. Saed and E. M. Terentjev, *Nat. Commun.*, 2022, **13**, 5753.
- 39 A. Duval, W. Benali and L. Avérous, *ChemSusChem*, 2025, **18**, e202401480.
- 40 R. Chen, L. Zhou, K. Zhang and M. Chen, *J. Appl. Polym. Sci.*, 2024, **141**, e55655.

View Article Online DOI: 10.1039/D5SU00828J

All data supporting the findings of this study are available. All the findings are included in the article and its supporting information. Full experimental procedures are provided in the supporting information.